

# Determination of the plastic behaviour of solid polymers at constant true strain rate

C. G'SELL\*, J. J. JONAS

*Department of Metallurgical Engineering, McGill University, 3450 University Street, Montreal, Quebec, H3A 2A7, Canada*

The methods of conventional tensile testing as applied to solid polymers are compared and reviewed critically. Experiments were performed using these techniques, and it is shown that large variations in local strain rate occur while necking and cold-drawing take place. A new tensile testing method is described in which the samples are tested at *constant local true strain rate*. This technique is based on the use of a diameter transducer, an exponential voltage generator and a closed-loop testing machine. Flow curves for poly(vinyl chloride) and high density polyethylene were determined at room temperature over the strain rate range of  $10^{-1}$  to  $10^{-4}$  sec $^{-1}$ . It is shown that the flow behaviour of these two polymers can be approximated by the constitutive relation:  $\sigma = K \cdot \exp [(\gamma_e/2)\epsilon^2] \cdot \dot{\epsilon}^m$ , where  $K$  and  $\gamma_e$  are constants and  $m$ , the rate sensitivity, is in the range 0.02 to 0.06. It is concluded that the positive curvature of the log  $\sigma$  flow curve is responsible for the stabilization of flow localization associated with cold drawing, and that the rate sensitivity plays a much smaller role.

## 1. Introduction

The tensile test performed with standard specimens at constant cross-head velocity has been widely used to investigate the mechanical properties of solid polymers. It makes possible the determination of engineering data (yield stress, maximum draw ratio, etc.) which are needed when these materials are employed in structural applications. However, the early occurrence of necking in these tests leads to difficulties in the physical interpretation of the quantities usually derived from the experimental data. The aim of this paper is two-fold: (i) we will first examine the limitations of the conventional testing techniques with respect to providing a rigorous description of the flow behaviour; (ii) we will then present a new testing method based on tensile testing at a constant true strain rate in a selected portion of the sample.

## 2. Conventional tensile testing and data processing

### 2.1. Review of common definitions for stress and strain

The specimens used in tensile tests by different workers have different shapes but all are characterized by their uniform cross-section  $A_0$ , in the calibrated portion of initial length,  $L_0$ . The cross-head velocity is normally kept constant, leading to a constant specimen elongation rate,  $\dot{L} = dL/dt$ . The primary data of all such tests are then the load,  $P$ , applied to the specimen and the corresponding elongation ( $L - L_0$ ). However, different approaches have been used to process these data and these are compared briefly below for the case of poly(vinyl chloride) (PVC) and high density polyethylene (HDPE). For example, Cross and Haward [1] report the load-extension curve as

\*Permanent address: Laboratoire de Physique du Solide, (L.A. au C.N.R.S. no 155), E.N.S.M.I.M., Parc de Saurupt, 54042 Nancy-Cedex, France.

obtained directly from the test. Alternatively, Oberst and Retting [2] and Andrews and Ward [3] divide the primary variables  $P$  and  $(L - L_0)$  by the initial cross-section,  $A_0$ , and length,  $L_0$ , respectively, and then display the “nominal stress” and “nominal strain”

$$\sigma_N = P/A_0, \quad \epsilon_N = (L - L_0)/L_0. \quad (1)$$

Still others, e.g. Jäckel [4], Lazurkin [5], Utsuo and Stein [6], Haward *et al.* [7], Pezzin *et al.* [8] label their curves “stress” and “strain” without precise definition of these terms, although these can be inferred to be nominal stress and strain.

Unfortunately, the conventional determination of tensile data and their presentation in the form of  $\sigma_N$  and  $\epsilon_N$ , while experimentally straightforward, do not adequately describe the physical behaviour of the material. The inadequacy arises first from the fact that, in this presentation, the load and elongation are referred, respectively, to the initial cross-section and length of the specimen and not to their current values. This leads to erroneous conclusions regarding the magnitude of yield drops, the rate of strain hardening, etc. On the assumption that the deformation is homogeneous or nearly homogeneous along the gauge length and that the specimen volume is constant, the above difficulty can be cleared up by using the following expressions to define the “homogeneous stress” and “homogeneous strain”

$$\sigma_H = P/A = (P/A_0) \cdot (L/L_0) = \sigma_N(1 + \epsilon_N) \quad (2)$$

$$\epsilon_H = \ln(L/L_0) = \ln(1 + \epsilon_N).$$

Here  $A$  and  $L$  are the current area of cross-section and length of the specimen. The above relations were used by Pampillo and Davis [9] and by Bahadur [10] in their investigations of the behaviour of PVC and HDPE and represent a first step towards the rigorous description of the flow of these materials.

However, due to the inhomogeneous nature of tensile flow in polymers (i.e. to the flow localization associated with necking and to the propagation of this localization along the specimen axis), the definitions given in Equations 2 cannot normally be applied to the deformation of PVC and HDPE. The occurrence of flow localization introduces two further inaccuracies, the first of which can be eliminated by defining the “true stress” and “true strain” in *local* terms as in

$$\sigma = P/A$$

$$\epsilon = \lim_{l_0 \rightarrow 0} [\ln(l/l_0)] \quad (3)$$

where  $l_0$  and  $l$  are the initial and current length of a small slice of the specimen located at the point where  $\sigma$  and  $\epsilon$  are defined. This was the approach used by Meinel and Peterlin [11], who determined the “true” flow curve of HDPE with the aid of a photographic technique. Their method involved the measurement of the mesh length of a very fine grid printed on the specimen prior to deformation. Because the strain could be considered to be homogeneous within a single mesh length, the local definition (Equations 3) of the strain was applied. For defining the true stress, these authors used the constant volume approximation and wrote  $\sigma = P/A_0 \cdot l/l_0$ .

The method of Meinel and Peterlin, while leading to the accurate determination of  $\sigma$  and  $\epsilon$ , has one remaining limitation, which is associated with the method of imposing the experimental strain rate. In conventional tensile testing, the cross-head speed remains constant, leading to the imposition of a constant nominal strain rate,  $\dot{\epsilon}_N$ , during the test. However, the propagation of flow localization during straining ensures that the particular elements undergoing necking are inevitably submitted to a higher local strain rate, while the rest of the sample is being strained at a much lower rate. Thus a single flow curve obtained by this technique will generally describe the flow behaviour of a polymer over a wide range of local strain rates (high while necking is taking place in the selected element; low while the neck is being propagated outside the chosen region).

Such a flow curve has obvious limitations with respect to the determination of the constitutive relation of the material. It also makes difficult the accurate measurement of the thermodynamic parameters associated with thermally activated flow. In the section to follow, we will describe some results obtained using conventional testing techniques, but which are reported in terms of the local relations given as Equations 3; in particular, the amount and nature of the strain rate variations during testing will be examined for the case of two selected PVC and HDPE polymers. We will then introduce a method of testing by means of which the local strain rate can be held constant; some typical results obtained by this technique will also

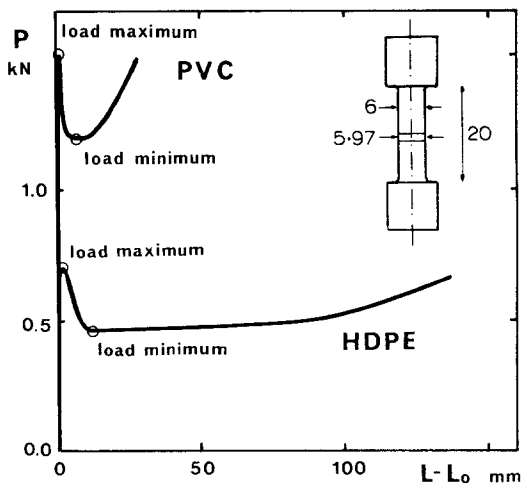


Figure 1 Load versus extension curves obtained in conventional tensile tests at constant cross-head velocity with cylindrical specimens of poly(vinyl chloride) (PVC) and high density polyethylene (HDPE). A small cross-section defect was machined in the centre of the specimens to induce necking at this location.

be presented and compared with those obtained by the previous methods.

## 2.2. Strain rate variations during the conventional tensile testing of PVC and HDPE

Samples of PVC\* and of high density PE (HDPE)<sup>†</sup> were prepared for tensile testing by machining to a gauge length of  $L_0 = 20$  mm and an initial diameter of  $D_0 = 6$  mm. Testing was carried out at room temperature ( $22 \pm 1^\circ \text{C}$ ) at a constant cross-head velocity of  $0.05 \text{ mm sec}^{-1}$ . The load-extension curves obtained in this way are displayed in Fig. 1. A significant load drop can be seen to occur in both materials, which is associated with neck formation at the central cross-section (the diameter of the sample was reduced by about 0.03 mm to induce necking at this location). The load drop is followed by a slow load increase, which is associated in turn with neck propagation along the specimen. A final load increase takes place when neck propagation is complete, leading to fracture.

In order to characterize the local response of the material, the diameter of the specimens at the central cross-section was measured continuously, leading to the diameter-extension curves of Fig. 2. They show that, for both polymers, most of the diameter reduction is achieved, not unexpectedly, during a brief initial part of the experiment. Nom-

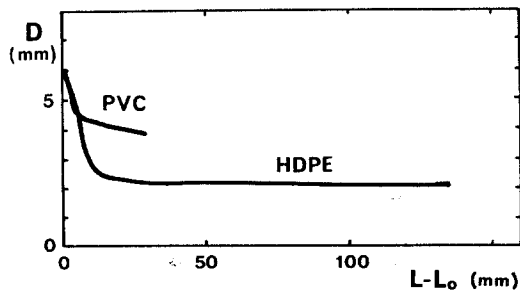


Figure 2 Dependence of the diameter in the centre of the specimen on the overall extension for the tests at constant cross-head velocity shown in Fig. 1.

inal stress-strain curves,  $\sigma_N/\epsilon_N$ , were calculated from the load-extension data by means of Equations 1 and are plotted in Fig. 3. The true stresses and strains were then calculated from the load and the diameter at the central cross-section. The true stress was obtained from Equations 3, whilst the true strain was derived from the diameter measurements by assuming the constant volume approximation and employing the relation

$$\epsilon = \ln(A_0/A) = 2 \ln(D_0/D). \quad (4)$$

The flow curves obtained in this way are displayed in Fig. 4.

It can be seen that the large yield drops displayed by the  $\sigma_N/\epsilon_N$  curves disappear when the data are converted to  $\sigma/\epsilon$  form. Instead, the flow stress increases continuously to fairly high values at failure. In terms of the mechanisms of deformation, the curves indicate that flow hardening is continuous and always positive.

As discussed above, the continuous measurement of local diameter (or local elongation) can permit the determination of a kind of "true" flow curve even though this curve does not give the response of the material to constant strain rate deformation. To illustrate this point, the evolution of the local true strain rate was deduced from the diameter-elongation (or time) measurements through Equation 4, and is plotted in Fig. 5 as a function of the local true strain  $\epsilon$ . It can be seen that the strain rate varied during the tests by a factor of about 20 for PVC and about 200 for HDPE. For comparison, we calculated the hypothetical homogeneous strain rate  $\dot{\epsilon}_H = d\epsilon_H/dt$  (plotted versus  $\epsilon$  in broken lines). The moment indicated in Fig. 5 by a circle when the neck strain

\*Poly(vinyl chloride): D101 Dark Grey from Carlew Chemicals Ltd.

<sup>†</sup>High density polyethylene: DFDY 6130 Natural 77 from Union Carbide Ltd.

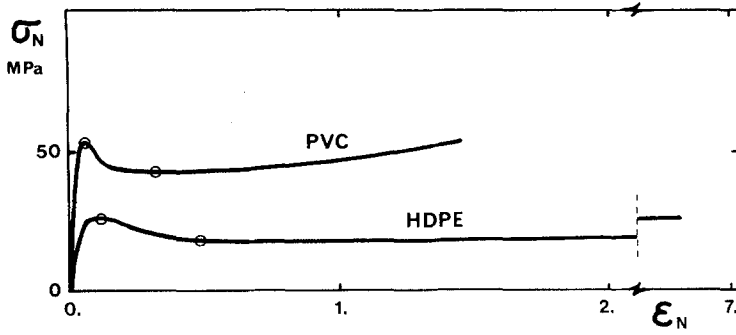


Figure 3 Nominal stress versus nominal strain curves for the tests of Fig. 1.

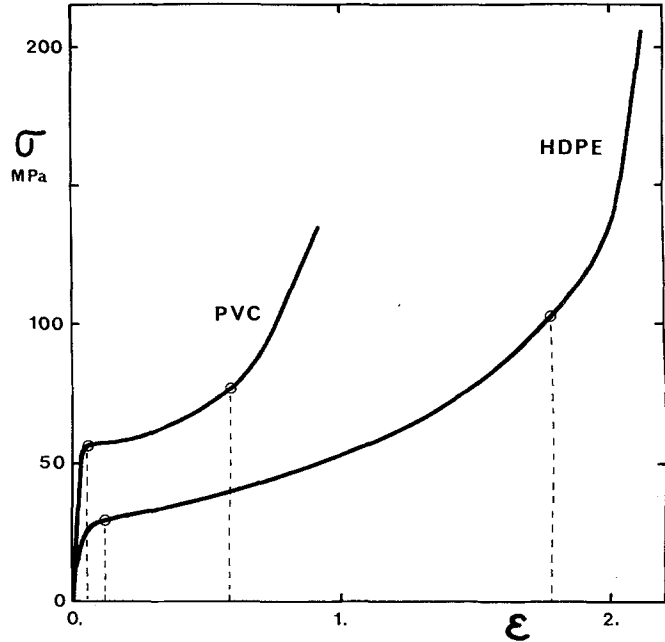


Figure 4 Local true stress versus local true strain in the centre of the specimen for the tests of Fig. 1.

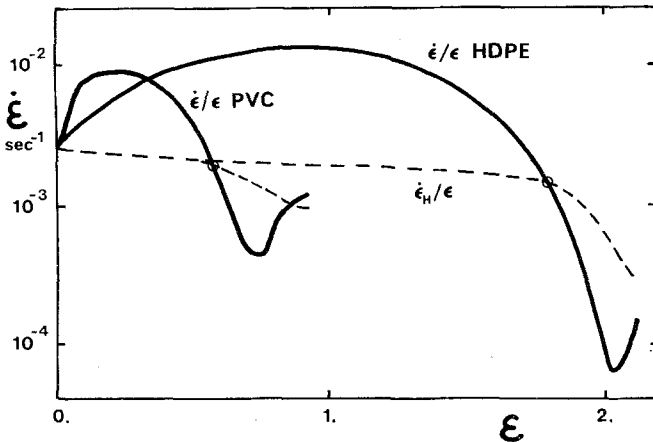


Figure 5 Dependence of the local true strain rate on local true strain in the centre of the specimen for the tests of Fig. 1. Note the logarithmic scale for the strain rate. The broken curves show the dependence of the hypothetical homogeneous strain rate  $\dot{\epsilon}_H$  (for definition, see Equation 2) on the local true strain in these constant cross-head speed experiments.

rate reattains the homogeneous value at the end of the period of neck formation corresponds to the point in time when the load minima are reached.

This one- to two-order of magnitude variation in strain rate which takes place during the determination of the flow curves of Fig. 4 and which is

illustrated in Fig. 5 prevents the data of the former figure from being useful for the quantitative description of the flow behaviour of these polymers or for the calculation of the strain-hardening coefficients. Instead, data for such purposes can be established at a constant true strain rate by means

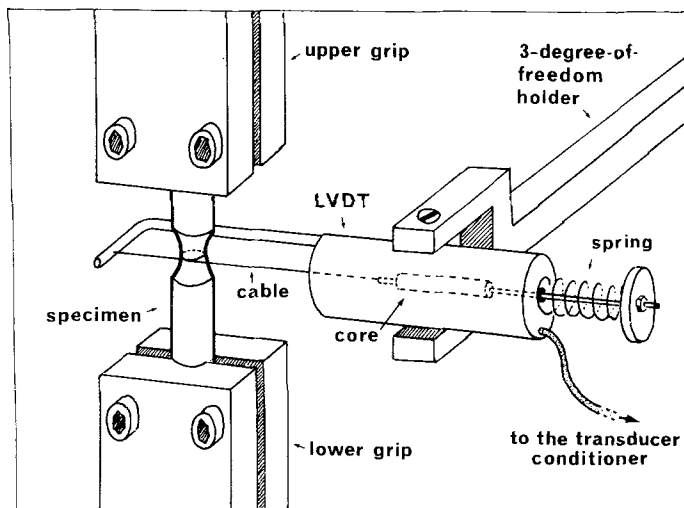


Figure 6 Schematic diagram of the circumference gauge used for continuously monitoring the diameter of the specimens.

of the apparatus and method to be described below.

### 3. A constant true strain rate testing method for polymers

#### 3.1. Apparatus and method

PVC and HDPE specimens were machined out of 12 mm diameter cylindrical rods to give an hour-glass shape with a minimum diameter of 6 mm. Tool bits with a radius of curvature of 5 mm were used for this purpose. The waisted specimens were attached to the grips of an MTS closed-loop tensile testing machine (Fig. 6). This type of equipment was selected for the present experiments because it has the capability of maintaining constant the true strain rate by controlling the cross-head velocity in an appropriate manner.

There are two elements in the necessary feedback control loop. The first is a specially designed circumferential gauge for measuring the neck diameter of the specimens. The circumference was monitored by means of a thin flexible steel cable wound once around the sample, the free end of the cable being attached to the core of a linear transducer (LVDT)\*. The d.c. output voltage,  $V_m$ , of the transducer (the "measured voltage") was adjusted to be proportional to the diameter of the sample: i.e.  $V_m = G(D_0 - D)$  where  $G$  is a gain factor.

The second key element in the feedback loop is the control voltage generator. As pointed out above, the true strain is given by  $\epsilon = 2 \ln(D_0/D)$  if the constant volume approximation is valid. Thus, the strain rate at any moment is  $\dot{\epsilon} = d[2 \ln(D_0/D)]/dt$  and, in order to keep it constant, the diameter must vary with time as  $D(t) = D_0 \exp(-\dot{\epsilon}t/2)$ . To this end, a control voltage is generated which varies with time as  $V_c(t) = GD_0[1 - \exp(-\dot{\epsilon}t/2)]$ . By manipulating the cross-head position in a suitable manner, the closed loop tensile machine ensures that the measured voltage continuously matches the control voltage. The latter is produced by an exponential operational amplifier coupled to the (linear) ramp generator of the MTS machine. A schematic diagram of this arrangement, which is accurate to within 0.1%, is shown in Fig. 7.†

#### 3.2. Experimental results

The materials tested at constant true strain rate were the same as those tested at constant cross-head velocity. Eighty experiments were performed at room temperature at constant true strain rates ranging from  $10^{-4}$  to  $10^{-1} \text{ sec}^{-1}$ . Some examples of the flow curves deduced from experimental load/diameter recordings are presented in Fig. 8. One can see that the flow curves determined at constant true strain rate are generally similar to

\*Because the circumferential transducer is sensitive to sticking friction between the cable and the specimen, during operation, a high frequency low amplitude vibration was applied to the sample by means of the "dither" adjustment on the MTS machine. This reduced the cable/specimen friction and the attendant instabilities to an acceptable level.

†It can be shown that a very close approximation of the exponential law  $V_c(t)$  is also obtained when the regular MTS sine function generator is used. For this purpose the frequency of the sine function must be set to  $f = 1.51 \times 10^{-1} \times \dot{\epsilon} \text{ sec}^{-1}$  and the sine amplitude adjusted with the span control to  $0.484 \times G \times D_0$ . This approximation is accurate to within 1% up to a true strain of 1.

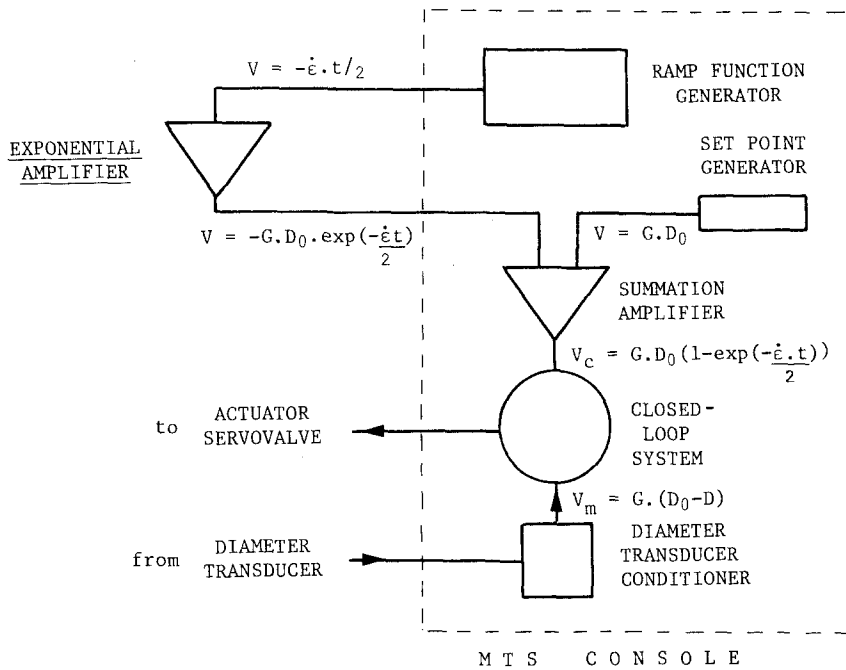


Figure 7 Equivalent electrical diagram of the exponential control voltage generator, diameter transducer and closed-loop system.

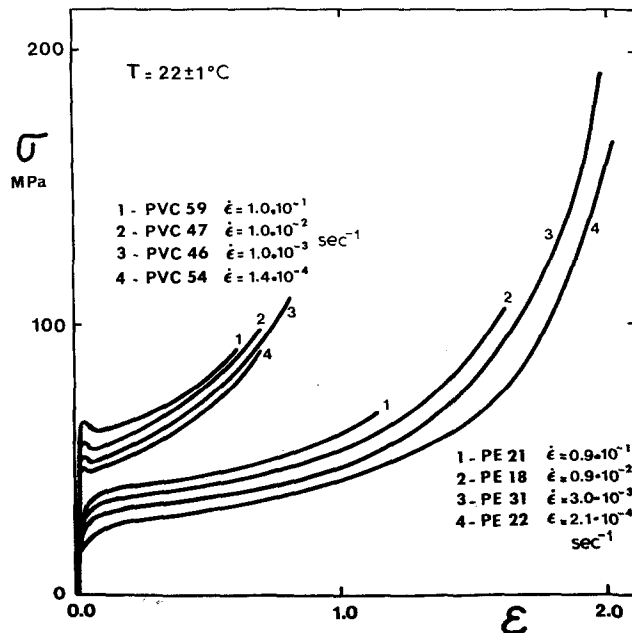


Figure 8 Typical true stress versus true strain curves obtained with hour-glass shaped specimens of PVC and HDPE tested at constant local true strain rate.

those determined at constant cross-head velocity (Fig. 4) in that they are characterized, apart from an eventual small yield drop, by a continuously increasing rate of strain-hardening. An important difference, however, is that the rate of increase in flow stress is greater at high strains in Fig. 8 than it is in Fig. 4. This is because the true strain rate is

held constant in the former and drops sharply in the latter case. Another interesting feature of the flow curves in Fig. 8 is the different yield behaviour of HDPE and PVC. While HDPE yields gradually without any sharp transition between the "elastic" and "plastic" regions, PVC exhibits a true yield drop when tested at constant true strain rate.\*

\*The true yield drop of PVC did not appear on the curves obtained at constant cross-head velocity because it was counterbalanced by the strain rate increase occurring simultaneously.

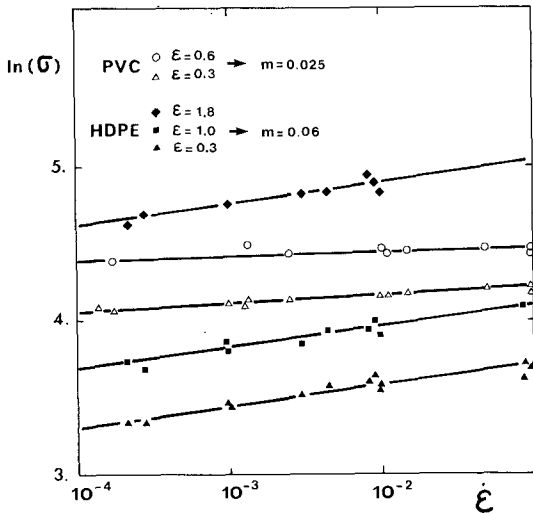


Figure 9 Examples of the  $\ln \sigma$  versus  $\ln \dot{\epsilon}$  linear regressions used to determine the strain rate sensitivity coefficient  $m = (d \ln \sigma / d \ln \dot{\epsilon})_{\epsilon}$  for PVC and HDPE.

## 4. Discussion

### 4.1. Constitutive equations of flow

One of the aims of this part of the investigation was to determine the constitutive relations  $\sigma(\epsilon, \dot{\epsilon})$  for the flow of the two polymeric materials. The flow curves determined by the present method were useful for this purpose, because the strain rate,  $\dot{\epsilon}$ , and strain  $\epsilon$ , are properly independent variables when the apparatus of Fig. 6 is used.

To evaluate the influence of  $\dot{\epsilon}$  on the flow stress, as commonly expressed through the strain rate sensitivity coefficient  $m = (d \ln \sigma / d \ln \dot{\epsilon})_{\epsilon}$ , a plot of  $\ln \sigma$  versus  $\ln \dot{\epsilon}$  was made, which is displayed in Fig. 9 for the two materials and for five selected values of  $\epsilon$ . It was found that, while  $m$  is nearly constant and equal to 0.06 for HDPE over the whole range of strain, the apparent rate sensi-

tivity of PVC decreases from 0.05 to nearly zero as the strain increases. This decrease in  $m$  is responsible for the convergence of the PVC flow curves over the strain rate range of Fig. 8. The apparent dependence of  $m$  on  $\epsilon$  in PVC can be attributed to the adiabatic temperature increase taking place when certain polymers are strained [12–14]. Although it has been shown [15] that an adiabatic effect is not responsible for the yield behaviour of these materials, it can reduce the flow stress at increasing strains and strain rates, and hence affect the apparent rate sensitivity. This conclusion is supported by the thermodynamic calculations of Hall [16] which indicate that the adiabatic temperature rise (and hence the probable variation of  $m$  with  $\epsilon$ ) is much smaller in HDPE than in PVC, because the thermal conductivity and the heat capacity of HDPE are respectively 3 and 2 times greater than those of PVC. The mean value  $m = 0.025$  adopted for PVC is, therefore, a measure of the mean actual rate sensitivity rather than an absolute isothermal strain rate sensitivity.

The influence of  $\epsilon$  on the flow stress can be expressed through the relative strain-hardening coefficient  $\gamma = (d \ln \sigma / d \epsilon)_{\dot{\epsilon}}$ . The curves obtained with both HDPE and PVC showed that  $\gamma$  increases with the strain. Therefore, a check was made to see if a first order dependence  $\gamma = \gamma_{\epsilon} \times \epsilon$  is valid. In such a case, and with a constant value of  $m$ , the flow curve  $\sigma(\epsilon, \dot{\epsilon})$  takes the simple form:

$$\sigma(\epsilon, \dot{\epsilon}) = K \exp\left(\frac{\gamma_{\epsilon}}{2} \cdot \epsilon^2\right) \cdot \dot{\epsilon}^m. \quad (5)$$

When this constitutive equation is obeyed, all the  $\sigma(\epsilon, \dot{\epsilon})$  data of a given polymer reduce to a single linear master curve in terms of  $\ln(\sigma/\dot{\epsilon}^m)$  versus  $\epsilon^2$ . Fig. 10 shows that, for HDPE and PVC, the master

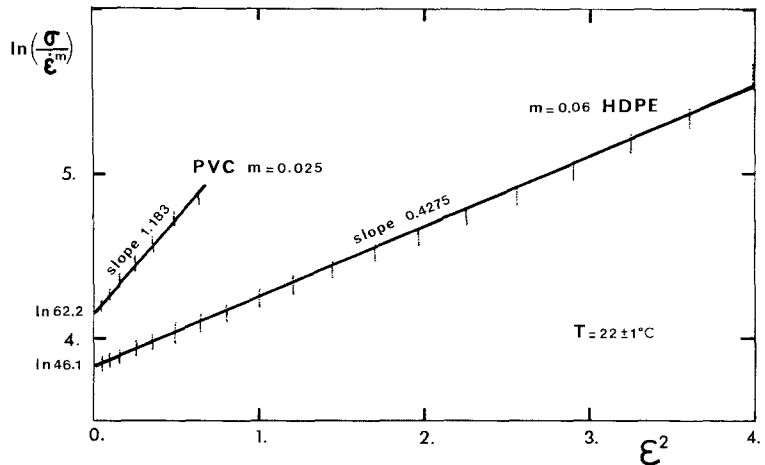


Figure 10 Master curves of the form  $\ln(\sigma/\dot{\epsilon}^m)$  versus  $\epsilon^2$  obtained with PVC and HDPE tested at constant true strain rate. The reasonable linearity of the master curves indicates that a constitutive relation of the type:  $\sigma = K \exp[(\gamma_{\epsilon}/2)\epsilon^2] \dot{\epsilon}^m$ , where  $K$ ,  $\gamma_{\epsilon}$  and  $m$  are material constants, is valid for these materials.

curve is reasonably linear, so that Equation 5 is valid within experimental error. From these fits, it is possible to deduce the constants  $K$  and  $\gamma_\epsilon$  and then to write the constitutive equations as follows:

$$\text{HDPE: } \sigma_{\text{MPa}} = 46.1 \exp(0.43 \epsilon^2) \cdot \dot{\epsilon}^{0.06} \quad (6)$$

$$\text{PVC: } \sigma_{\text{MPa}} = 62.2 \exp(1.18 \epsilon^2) \cdot \dot{\epsilon}^{0.025}.$$

It is clear that these equations tend toward definite non-zero values  $K \dot{\epsilon}^m$  as  $\epsilon$  tends toward zero. They therefore represent the steady plastic flow behaviour of the material and not the initial “elastic” region, nor the detailed behaviour in the yield region. This initial loading behaviour will form the subject of a separate publication [17].

The unexpectedly low values of the strain rate sensitivity coefficients,  $m$ , of the same order as for metals at room temperature, show that the stabilization of the flow localization (which leads to the transition from necking to cold-drawing) is not due to a strain rate effect, but can be attributed, as predicted by Ward [18], to the positive curvature of the  $\log \sigma$  flow curve. In the present two materials, this curvature can be described by a linear dependence of the strain-hardening coefficient  $\gamma$  upon strain.

#### 4.2. Limitations of the present technique

The definition used for the stress in the central part of the specimens (Equations 3) was expressed entirely in terms of the two recorded variables  $P$  and  $D$  (or  $A$ ). However, it is known that when a tensile specimen does not have a perfectly uniform cross-section, radial stresses are developed which create a triaxial state of stress. Bridgman [19], in a somewhat simplified mechanical approach, showed that the true axial stress can be deduced from the measured stress by reducing it by a correction factor. This factor depends on the ratio  $a/R$  of the cross-sectional radius,  $a$ , to the radius of curvature of the neck profile,  $R$ . Although Thomason [20] found that the Bridgman correction factor overestimates the effect of triaxiality, in the present work it has been observed to be valid, to a reasonable approximation. Nevertheless, the experimental curves were not corrected by this factor because, due to the evolution of flow localization, the profile of the specimens was continuously changing during the tests. It should be noted that, with the present “hour-glass radius” of 5 mm, the Bridgman factor was about 0.9 at the beginning of the tests and close to 1 at failure (the necked region having at that stage a locally uniform cross-

section). The corrections appropriate to the early part of the flow curve can be reduced by using a larger “hour-glass radius”: e.g. 10 mm. This was done for some of the tests, but only leads to a small change in the coefficients of the constitutive relations (Equations 6 above), and does not, of course, affect the principal physical conclusions.

It was seen above that, unlike the HDPE specimens, the PVC specimens show a small but significant true stress drop in the constant true strain rate experiments. As pointed out earlier by Brown and Ward [21], this true stress drop is a transient effect due to the difference between the conditions for the initiation and the propagation of yielding in glassy polymers. It has no influence on the rest of the curve. There is, however, some evidence [17] that the initial stress drop in PVC is associated with *inverse* stress transients when rapid strain rate changes are performed. By contrast, the absence of a yield drop in HDPE is linked with the presence of *normal* stress transients.

It remains to add that, in the method of constant true strain rate testing described above, a question can arise regarding the basic assumption that the volume remains constant during straining. Although it has been shown experimentally [11, 22] that the total change of volume during the plastic deformation of cold-drawable polymers is less than 1% (that is, that the plastic Poisson ratio  $\nu_{\text{pl}} \approx 0.5$ ), it is known that the constant volume approximation does not hold for the elastic part of the strain (for which  $\nu_{\text{el}} \approx 0.3 - 0.4$ ). We can therefore write the total true strain as

$$\begin{aligned} \epsilon_{\text{total}} &= \epsilon_{\text{el}} + \epsilon_{\text{pl}} \\ &= \sigma/E + (2 \ln(D_0/D) - 2\nu_{\text{el}} \sigma/E), \end{aligned} \quad (7)$$

where  $E$  is the elastic modulus. It can be seen that  $\epsilon_{\text{total}}$  differs by the small correction term  $(1 - 2\nu_{\text{el}}) \sigma/E$  from the expression  $\epsilon = 2 \ln(D_0/D)$  used in the current method for defining the true strain, and that  $\epsilon_{\text{pl}}$  differs by  $-2\nu_{\text{el}} \sigma/E$ . As an illustration of this point, the values of  $\epsilon_{\text{total}}$  and  $\epsilon_{\text{pl}}$  are plotted in Fig. 11 as a function of  $\epsilon = 2 \ln(D_0/D)$  for the case of a PVC specimen ( $\dot{\epsilon} = 10^{-4} \text{ sec}^{-1}$ ). The relative error in  $\epsilon$  (and hence in  $\dot{\epsilon}$ ) is seen to be small and to decrease as  $\epsilon$  increases. This small error cannot be corrected using the current device, but can be eliminated if the testing machine is interfaced with a suitable computer. In the latter case, it is possible to perform tensile tests at a constant true *plastic* strain rate. This is

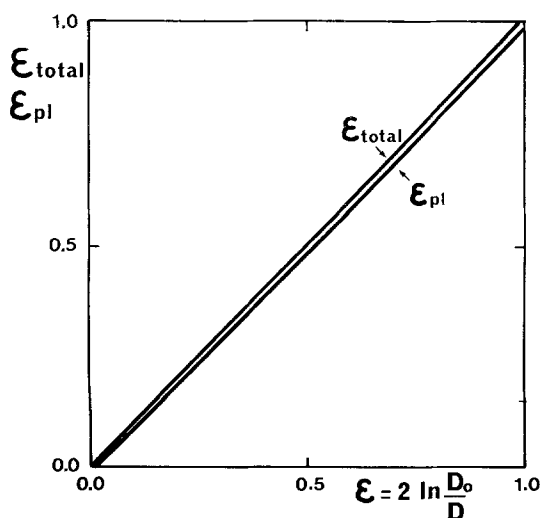


Figure 11 Divergence of the total strain  $\epsilon_{\text{total}}$  and the plastic strain  $\epsilon_{\text{pl}}$  from the calculated strain  $\epsilon = 2 \ln(D_0/D)$  because of the small variation in volume associated with the elastic component of the strain ( $\nu \neq 0.5$ ).

not expected to change the overall behaviour depicted in Fig 8, but is likely to increase the initial yield drop when it is observed (e.g. in PVC).

## 5. Conclusions

(1) The nominal stress–strain curve obtained from the conventional tensile test does not reflect the local flow behaviour of solid polymers. This is because, during a test at constant cross-head velocity, the local true strain rate exhibits very large variations.

(2) Constant true strain rate–flow curves can nevertheless be obtained with the aid of the procedure described above. This is based on the use of a specimen circumference transducer, an exponential function generator, and a closed-loop testing machine.

(3) The flow curves of PVC and HDPE were determined in this way at room temperature. The curves can be approximated by a constitutive equation of the form:

$$\sigma = K \cdot \exp\left(\frac{\gamma\epsilon}{2} \cdot \epsilon^2\right) \cdot \dot{\epsilon}^m,$$

where  $K$ ,  $\gamma\epsilon$  and  $m$  are constants.

(4) The present solid polymers are characterized by: (i) a very low strain rate sensitivity coefficient  $m \leq 0.06$ ; and (ii) a high relative strain-hardening coefficient  $\gamma$ , which is proportional to strain.

(5) The stabilization of plastic instability (i.e. the propagation of the neck during the cold-drawing process) is not due to the increase in local strain rate, but to the positive curvature of the flow curve.

## Acknowledgements

The authors are indebted to the National Research Council of Canada and to the Ministry of Education of Quebec (FCAC program) for financial support. C. G'Sell expresses his gratitude to the Institut National Polytechnique de Lorraine for a period of sabbatical leave and to the Ministry of Inter-governmental Affairs of Quebec for the award of a France–Quebec Research Fellowship.

## References

1. A. CROSS and R. N. HAWARD, *J. Polymer Sci.* **11** (1973) 2423.
2. H. OBERST and W. RETTING, *J. Macromol. Sci.-Phys.* **B5(3)** (1971) 559.
3. J. M. ANDREWS and I. M. WARD, *J. Mater. Sci.* **5** (1970) 411.
4. K. JÄCKEL, *Kolloid Z.* **137** (1954) 130.
5. YU. S. LAZURKIN, *J. Polymer Sci.* **30** (1958) 595.
6. A. UTSUO and R. S. STEIN, *ibid.* **5** (1967) 583.
7. R. N. HAWARD, B. M. MURPHY and E. F. T. WHITE, *ibid.* **A2-9** (1971), 801.
8. G. PEZZIN, G. AJROLDI, T. CASIRAGHI, C. GARBUGLIO and G. VITTADINI, *J. Appl. Polymer Sci.* **16** (1972) 1839.
9. C. A. PAMPILLO and L. A. DAVIS, *J. Appl. Phys.* **43** (1972) 4277.
10. S. BAHADUR, *Polymer Eng. Sci.* **13** (1973) 266.
11. G. MEINEL and A. PETERLIN, *J. Polymer Sci.* **A2-9** (1971) 67.
12. F. H. MÜLLER and K. JÄCKEL, *Kolloid Z.* **129** (1952) 145.
13. P. BRAUER and F. H. MÜLLER, *ibid.* **135** (1954) 65.
14. I. MARSHALL and A. B. THOMPSON, *J. Appl. Chem.* **4** (1954) 145.
15. P. I. VINCENT, *Polymer* **1** (1960) 7.
16. I. H. HALL, *J. Appl. Polymer Sci.* **12** (1968) 739.
17. C. G'SELL and J. J. JONAS, to be published.
18. I. M. WARD, "Mechanical Properties of Solid Polymers" (Wiley-Interscience, London, 1971) p. 275.
19. P. W. BRIDGMAN, *Trans. Amer. Soc. Met.* **32** (1944) 553.
20. P. F. THOMASON, *Int. J. Mech. Sci.* **11** (1969) 481.
21. N. BROWN and I. M. WARD, *J. Polymer Sci.* **A2-6** (1968) 607.
22. Y. WADA and A. NAKAYAMA, *J. Appl. Polymer Sci.* **15** (1971) 183.

Received 21 April and accepted 20 July 1978.